www.jchr.org

JCHR (2021) 11(4), 474-488 | ISSN:2251-6727



Synthesis of Quinoxalines and Benzimidazole Derivatives by Citrate Sol-Gel Auto-combustion Synthesized CoFeMnO₄ Nanoparticles.

Uttam D. Kadam, Satyanarayan M. Arde, Rajkumar S. Pandav, Sanchita P. Patil , Rahul D. Gharage, Bajirao S. Shirke *

Department of Chemistry, Yashwantrao Chavan Warana Mahavidyalaya, Warananagar, Affiliated to Shivaji University, Kolhapur 416113, (MS, India).

*Corresponding author e-mail-,<u>bss_chemistry@yahoo.com</u>, Tel.: +91 02328 224041.

Contributing author e-mails: uttamkadam123@gmail.com satyanarayan.arde2520@gmail.com,

rajkumarpandav@gmail.com, sanchitaukadam@gmail.com, rahul1911995@gmail.com

(**Received**: 14 January 2021 **Revised**: 01 February 2021 **Accepted**: 18 March 2021)

KEYWORDS

ABSTRACT:

Citrate Sol-Gel auto combustion, Spinel Lattice,
Stoichiometry,
Manganese substituted Cobalt Ferrite, Catalytic Activity,
Quinoxalines and Benzimidazole derivatives,
Magnetic nature.

Formation of manganese doped cobalt ferrite nanoparticles with the chemical composition CoFeMnO4 was synthesized by the citrate sol-gel auto combustion method. Thermal analysis of as prepared sample was carried out by TG-DTA. The crystal structure, morphological analysis and size of particle were investigated by using X-ray diffraction (XRD) study, Fourier Transform Infrared Spectrometer (FTIR) Scanning Electron Microscopy (SEM) and Transmission Electron Microscopy (TEM) techniques. Magnetic character of synthesized nanomaterials was investigated by Vibrating Sample Magnetometer (VSM) Study. The X-ray diffraction pattern confirms a single phase cubic spinel structure whereas, FT-IR study further supports spinel structure adopted by catalyst synthesized and TEM study reveals formation of nanosized material synthesized by method adopted. Elemental analysis as obtained by EDAX is in close agreement with the expected composition. VSM study reveals ferromagnetic nature of nanoparticles. Well characterized nanomaterials were used in the syntheses of medicinally important quinoxalines and benzimidazole derivatives and catalyst could be recycled up to five cycles with modest change in catalytic activity.

1. **Introduction**

Spinel ferrites have a great attention in researchers regarding to their extra ordinary electronic, magnetic, chemical, mechanical and thermal properties. These properties are largely influenced by their particle dimensions. Ferrites have practical structures applications in energy storage and conversion [1], magnetic-electric [2], ferro-fluid technology Biomedical, Photocatalysis, Sensors and Radars [4]. Properties of these materials modified by their chemical composition, microstructure and the synthesis method selected. They have the general formula AB2O4where A is generally divalent cation and B is trivalent cation occupying tetrahedral and octahedral sites respectively. In inverse spinel, cation B substitutes cation A. The unit cell contains 32 oxygen atoms in cubic cross-link packing with 8 tetrahedral (Td) and 16 octahedral (Oh) occupied sites. Altering the trivalent in the ferrites, enable us to obtain a large range of different physical and chemical properties [5].

The Spinels can be synthesized by different chemical methods like chemical co-precipitation [6], sol-gel [7], hydrothermal solvothermal [9], thermal [8], decomposition [10] and microwave combustion methods [11]. These wet chemical methods are economic, easy, requires less time and low temperature, produces particles of nanometer dimensions and therefore now a day's commonly used in the synthesis of nanoparticles. But sol-gel method offers several advantages over other synthesis methods, for the preparation of mixed metal oxides having spinel structures like precise control in composition and homogeneity forming material with desired stoichiometry. Sol-gel method operates at relatively lower temperature and this lower processing temperature is advantageous for avoiding phase segregation and reducing energy consumption. This method works at mild pH environment. Sol-gel chemistry inherently produces porous material enhancing the material's surface area, accessibility of active sites,

www.jchr.org

JCHR (2021) 11(4), 474-488 | ISSN:2251-6727



and diffusion properties, which are beneficial for catalytic applications [12].

Nanoscale spinel type mixed oxides have been extensively studied in the last few years due to their high thermal resistance and specific catalytic and electronic properties. Preparation method, precursor compounds, molar ratios, thermal treatment, and the presence of doping are important factors affect the performance and the properties of ferrites. Spinel nanoparticles of cobalt and manganese ferrites gained attraction of investors due to their outstanding magnetic and catalytic properties. They have wide applications in various sectors such as surface chemistry and catalysis. These types of catalysts have the advantages of environmental friendliness, easy magnetic separation, and low cost. [13-17].

Quinoxaline heterocyclic skeleton is present in many bioactive [18] and optoelectronic [19] compounds. Benzimidazole nucleus is the most important scaffolds due to their medicinal properties [20] and found in a number of naturally occurring compounds such as histamine, histidine, pilocarpine, allantoin and vitamin B_{12} [21]. In this regard, in the present research, we tuned the catalytic properties of manganese substituted cobalt ferrite to better catalyst for organic transformation reaction. The physical properties of CoFeMnO₄ strongly depend on substituting materials, annealing temperature, grain size, and also on the synthesis method. The replacement of iron by manganese ions in cobalt ferrites can alter magnetic behaviors, which makes them suitable for catalytic applications. The prime purpose of the work reported here is to study the Synthesis of Quinoxalines and Benzimidazole Derivatives by using manganese doped cobalt ferrites. For this the catalyst CoFeMnO₄ is produced and studied. The aim of present investigation is to synthesize the manganese substituted cobalt ferrite nanoparticles by using citrate sol-gel auto combustion its characterization using sophisticated method. analytical techniques and catalytic activity in the synthesis of medicinally important of N-heterocyclic compounds.

2. Experimental details

2.1 General procedure for the synthesis of CoFeMnO₄

Analytical grade Cobalt nitrate $[Co(NO_3)_2.6H_2O]$, Iron nitrate $[Fe(NO_3)_3.9H_2O]$, Manganese nitrate $[Mn(NO_3)_2.4H_2O]$ and citric acid $[C_6H_8O_7.H_2O]$ were selected in stoichiometric quantities to prepare

CoFeMnO₄. Method selected for synthesis of material was citrate sol-gel auto combustion. Metal nitrates and citric acid were dissolved in minimum quantity of deionized water with 1:1 molar ratio. The pH of the solution was adjusted to about 9.0 to 9.5 using ammonia solution. The solution was transformed to dry gel on heating to 353 K. On further heating the dried gel converts in a self propagating combustion manner until all the gel completely converted to a floopy powder. The as prepared precursor powder was pre-sintered at 673 K for 1 h then sintered at 1073 K for 5 h for confirmation of phase formation.

General procedure for the synthesis of Quinoxaline/ Imidazole

A 100 ml round bottom flask was charged with a mixture of Benzil/aldehyde (1 mmol), ortho phenyl diamine (OPD) (1 mmol) and 1 mol% of CoFeMnO₄. The mixture was stirred in water at room temperature (31°C) about 5-10 minute. The completion of reaction was monitored by TLC and solid separated by filtration on pouring the mixture into ice cold water. The obtained product was recrystallized in ethanol to afford the pure product.

2.1 Characterization

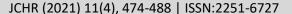
The phase formation of the sintered sample was confirmed by x-ray diffraction studies. The powder XRD pattern was recorded on a Philips PW-1710 x-ray diffractometer using CuK α radiation (λ =1.5406Å). Thermal analysis of precursor after auto-combustion was carried out by TG-DTA. Elemental analysis and surface morphology were analyzed by EDAX spectroscopy and scanning electron microscope (SEM: Model JEOL-JSM6360), particle size was measured using a transmission electron microscope (TEM) (Phillips CM 200, operating voltage 20-200kV). The room temperature magnetic measurement for the composition was performed by using a computerized high field vibrating sample magnetometer up to 15 kOe applied magnetic field.

3. Results and discussion

3.1 Thermal analysis

Thermal analysis was studied by using as synthesized precursor from 10 $^{\circ}$ C to 1000 $^{\circ}$ C in air atmosphere at the heating rate of 10 $^{\circ}$ C /min and it is shown in Fig. 1.

www.jchr.org





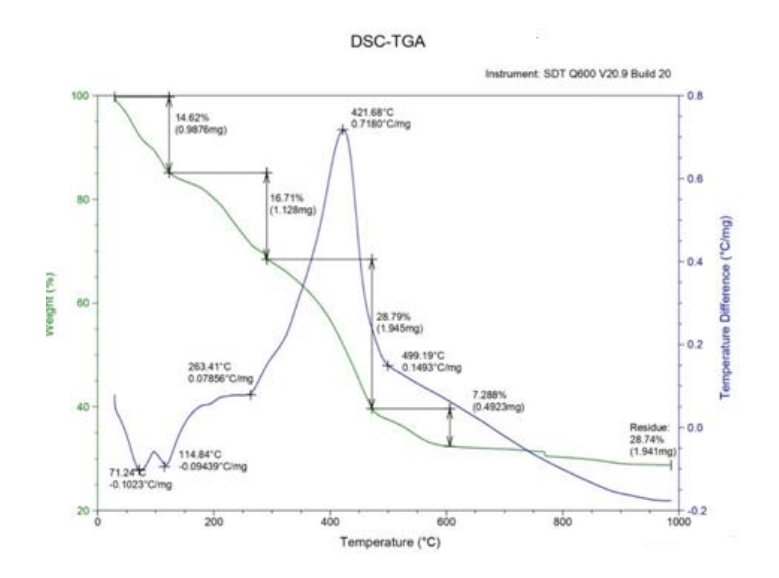


Fig.1. TGA-DTA curves for CoFeMnO₄ sample.

The TG curve shows that the initial sample losses are about 14.62% weight of its original weight observed by the removal of absorbed water and water of crystallization up to ~115 °C. An exothermic peak at about 421.68 °C was observed due to the evolution of heat by the removal of absorbed water and water of crystallization. The decomposition of citrate complex was started from 270 °C and it was completed at 499.1 °C. During this decomposition the sample looses 28.79 % weight. The DTA curve shows the formation of spinel

oxide at about 500 °C. This weight loss corresponds to the decomposition of carbonaceous and nitrogenous material present in synthesized powder with the liberation of CO₂, NO_x etc. After 800 °C samples do not show any further weight loss and attain stability [22].

X-ray diffraction study

Typical X-Ray diffraction pattern of sample CoFeMnO₄ obtained by citrate sol-gel auto combustion method followed by annealing at 1073 K is shown in Fig. 2

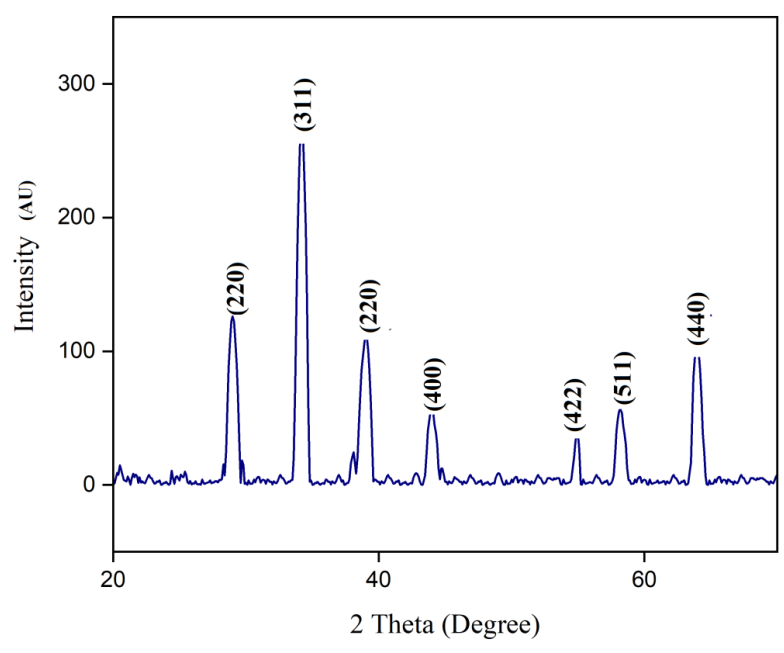


Fig. 2 X-ray diffraction patterns of CoFeMnO₄ sample

www.jchr.org

JCHR (2021) 11(4), 474-488 | ISSN:2251-6727



The X-ray diffraction pattern, for the CoFeMnO₄, synthesized by the citrate sol gel method show single-phase spinel structure. Diffraction peaks at planes of (220), (311), (222), (400), (422), and (511) in the XRD diffractograms reveals formation of typical cubic spinel structure. XRD peaks for CoMnFeO₄ are indexed and good close agreement to the standard pattern reported in the JCPDS card no. 00-001-1121 [23].

The particle size was calculated from XRD data using Scherrer formula.

$$t = 0.9 \lambda / \beta \cos \theta \tag{1}$$

Where, symbols t = crystallite size, $\lambda = \text{wave length of X-ray}$, $\beta = \text{full width at half maximum and } \theta = \text{Bragg}$ angle. Calculated vale of particle size from XRD is 37 nm, due this material is formed with higher surface area with advantage of porosity of citrate sol gel method.

3.3 FT-IR Study

The IR absorption spectra were recorded in the range 500-2000 cm⁻¹ shown in Fig.3.

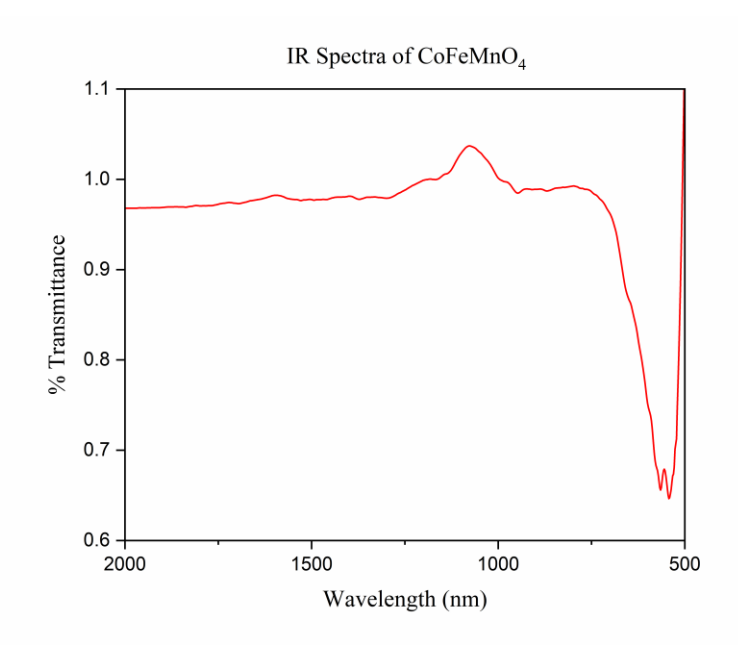


Fig.3 IR spectra of CoFeMnO₄ sample

FTIR spectroscopy is used for identifying the various functional groups as well as the stretching and bending vibrations of tetrahedral and octahedral complexes in spinel structure. FTIR spectrum of CoFeMnO₄ was carried out using Perkin Elmer Spectrometer with KBr pellet technique and shown in Fig. 3. The Figure revealed that the formation of pure nanoparticles without any major impurities. Two main absorption bands were observed below 1000 cm⁻¹. IR peak observed around 647 cm⁻¹ is due to stretching vibrations of M-O bond in the tetrahedral sites. Peak at 538 cm⁻¹ belongs to the bending

M-O vibration in octahedral site. Peak at 538 cm⁻¹ complements peak at 647 cm⁻¹ confirming spinel structure. [24]

3.4 Scanning electron microscopy

The surface morphology of CoFeMnO₄ was examined by scanning electron microscopy. Typical micrograph of the sample treated at 1073 K for 5 h is shown in Fig.4. All the crystallites were having different morphological structure with different dimensions. The size determined from SEM is below 40 nm.

www.jchr.org

JCHR (2021) 11(4), 474-488 | ISSN:2251-6727



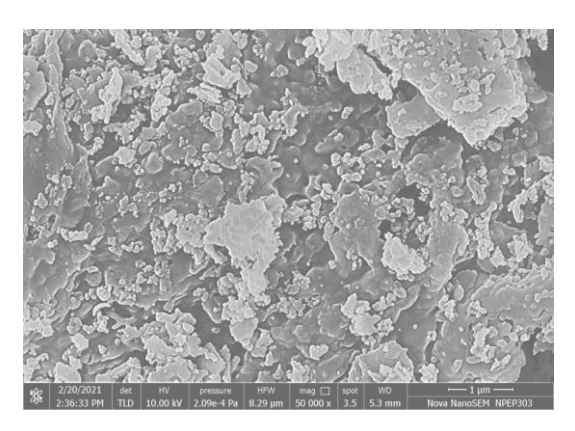


Fig.4 SEM images of CoFeMnO₄ sample

3.5 Energy dispersion x-ray analysis The composition of the nanocrystalline manganese substituted cobalt ferrite was determined using the Energy dispersive X-ray

analysis (EDAX). The Results of EDs analysis spectrum of sample is shown in Fig 5. The presence of Co, Mn and Fe in the sample is confirmed from EDS analysis.

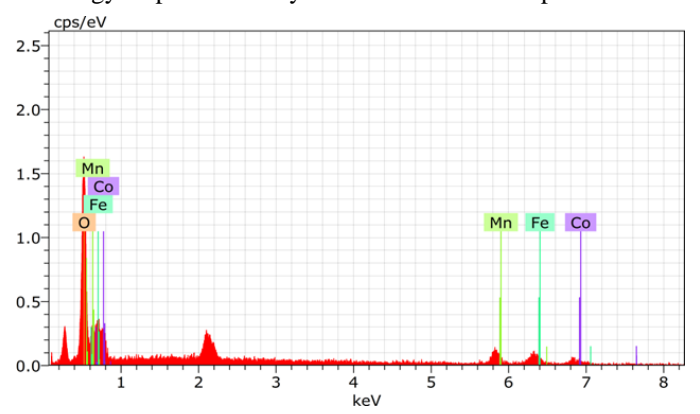


Fig.5 EDS patterns for the system CoFeMnO₄ sample

Theoretical values for Co, Fe and Mn are 33.33 % for all Co, Fe and Mn, EDX analysis provided results are 33.86, 32.27 and 32.87 % respectively. The quantitative analysis of the EDAX spectrum revealed the relative atomic ratio of all elements is close to the expected values for theoretical values.

TEM reveals detailed structural information at the atomic and nanometer scales. Typical TEM image of $CoFeMnO_4$ sample was shown in Fig 6 and it was confirmed that all particles are uniform and the grain size is ~37 nm in good agreement with value obtained from XRD.

3.6 Transmission electron microscopy

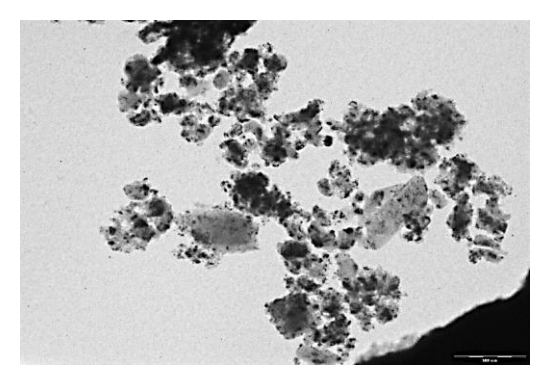


Fig. 6 TEM image for CoFeMnO₄

www.jchr.org

JCHR (2021) 11(4), 474-488 | ISSN:2251-6727



3.7. Magnetic Study

The magnetic properties of Manganese substituted cobalt ferrite sample was recorded by using hysteresis loop technique at room temperature with the applied field of 15 kOe in VSM instrument, is shown in Fig.7. The magnetic hysteresis (M-H) loop confirms that the

sample possess ferromagnetic performance with soft magnetic nature with considerable coercivity. From the results it is observed that saturation magnetization, coercivity, and remanent magnetization is less than typical cobalt ferrites due to substitution of manganese in the crystal lattice [25-26].

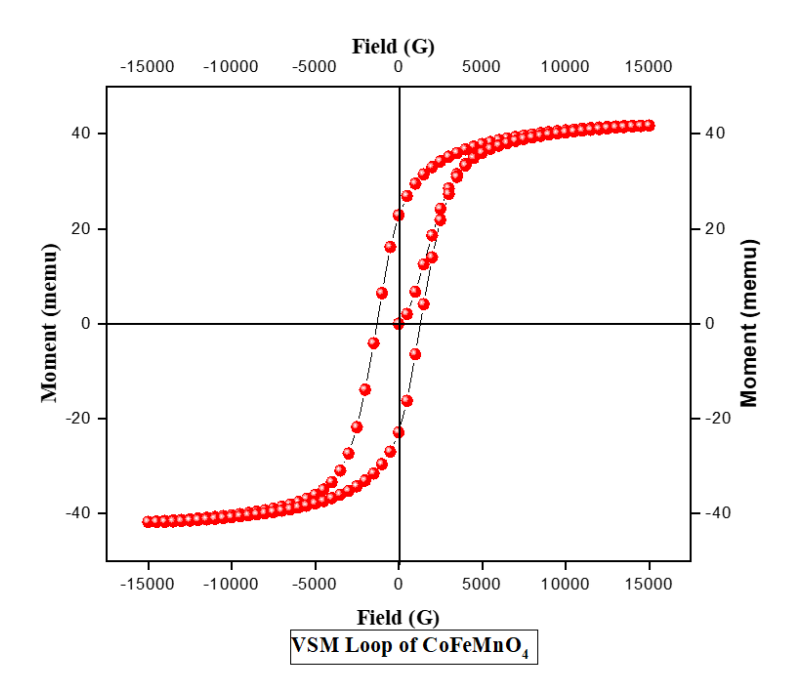


Fig. 7 VSM plots for CoFeMnO₄ sample.

With the above characterization, catalytic activity of CoFeMnO₄ has explored for the synthesis of biological active N-heterocyclic compounds namely quinoxalines and benzimidazole derivatives in water at room temperature. As aqueous media propose many practical and economic advantages, ecological advantages and greenness of water, it is beneficial to use as a reaction solvent because it is safe, harmless, and environmentally friendly [27].

Catalytic activity of CoFeMnO₄ firstly tested with the synthesis of quinoxaline. The condensation reaction of benzil with orthophenylenediamine (OPD) was used as a model reaction to investigate the catalytic performance of CoFeMnO₄ and the effect of media upon the reaction.

In the absence of catalyst the product 3a (Table 4, entry 1) was produced with very trace amount after 10 h of stirring in water (Table 1, entry 1), but on addition of CoFeMnO₄ (1mol % in comparison with the other reported catalyst) [28] in reaction mixture, conversion of substrate to product was suddenly increased up 98% in 10 min (Table 1, entry 6). There is a noticeable difference in the product yield between water and organic solvent. This might be due to dispersion of catalyst in the solvent. Synthesized CoFeMnO₄ was crystalline in nature (Figure 2) and well dispersed in the water whereas in organic solvent it was aggregated and settled down. This might be the reason that the yield of the product is low in organic solvent as compared to water.

www.jchr.org

JCHR (2021) 11(4), 474-488 | ISSN:2251-6727



Scheme 1

Table 1: Optimization studies for the synthesis of quinoxaline

Sr.No.	Reaction medium	CoFeMnO ₄ (mol %)	Time	Reaction	Yield ^b (%)
				condition	
1	H_2O	-	10 h	r.t./reflux	Trace
2	C_2H_5OH	-	10 h	r.t./reflux	Trace
3	CH ₃ CN	-	10 h	r.t./reflux	Trace
4	DMF	-	10 h	r.t./reflux	Trace
5	Acetone	-	10 h	r.t./reflux	Trace
6	H_2O	1	10 min	r.t.	98
7	$C_2H_5OH:H_2O$ (1:1)	5	15 min	r.t.	95
8	C_2H_5OH	5	20 min	r.t.	81
9	Acetone	5	20 min	r.t.	80
10	Acetone: $H_2O(1:1)$	5	15 min	r.t.	90
11	DMF	5	20 min	r.t.	68
12	CH₃CN	5	30 min	r.t.	60

^aReaction conditions: Benzil (1.0 mmol), *o*-phenylenediamine (1.0 mmol), Solvent (5 mL), CoFeMnO₄ (catalyticamount). ^bIsolated yield.

With these results in hand, we have determined the CoFeMnO₄ concentration for maximum yield of the product in water. Thus, the model reaction was carried out with various concentrations (mol %) of CoFeMnO₄ in water at ambient temperature. By changing concentration, dramatic effect on the conversion rate of

quinoxaline has been observed. As shown in, linear relationship was observed with concentration. The yield of the product is highest at 1mol % of CoFeMnO₄ catalyst. On the other hand, further increase in concentration resulted in no increase or decrease in the product yield.

Table 2: Optimization of catalyst for quinoxaline synthesis^a

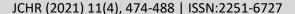
Entry	Catalyst (mol %)	Time (min)	Yield ^b (%)
1	0.2	45	40
2	0.4	25	52
3	0.6	15	75
4	0.8	15	84
5	1.0	10	98
6	1.2	10	98

^aReaction conditions: *o*-phenylenediamine (1.0 mmol), Benzil (1.0 mmol), Water (5 mL), RT. ^bIsolated yields after purification.

For practical applications of heterogeneous systems, the lifetime of the catalyst and its level of reusability are very important features. The recyclability of catalyst was

investigated with consecutive quinoxaline synthesis by taking o-phenylenediamine (1.0 mmol), Benzil (1.0 mmol) in aqueous medium at room temperature. After

www.jchr.org





the completion of first cycle, the product was extracted by ethyl acetate and the catalyst was recovered by strong magnet and extensively washed with water, dichloromethane, and acetone. The catalyst was then dried under vacuum before performing the reusability test. The recycling results of catalyst were summarized in Table 3. After the first cycle activity of catalyst is decreased with decreasing yield from 98 to 84 % with increased time.

Table 3: Recyclability of catalyst in quinoxaline synthesis

Entry	o-phenylenediamine	Cycle	Time (min)	Yield (%)
		1	10	98
	\sim NH ₂	2	15	97
1		3	18	94
	NH ₂	4	20	91
		5	25	88
		6	25	84

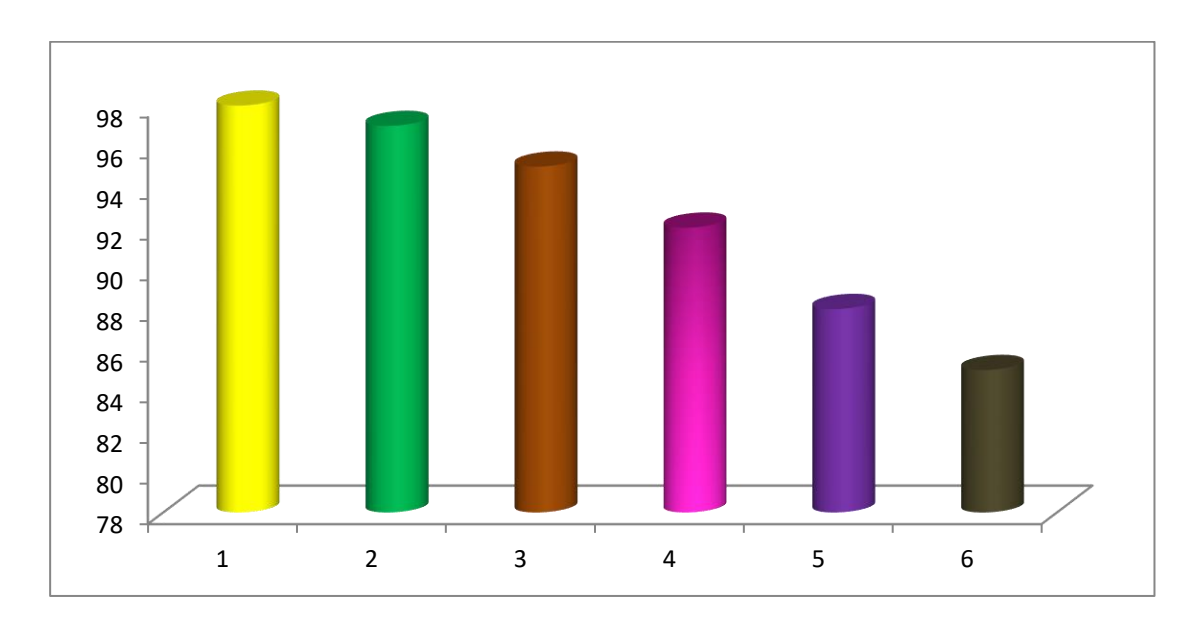


Figure 8: Graphical representation reusability of CoFeMnO₄ catalyst in quinoxaline synthesis

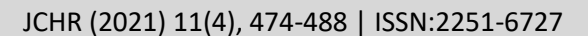
To explore the scope and generality of the catalyst, the optimized protocol [*o*-phenylenediamine (1.0 mmol), Benzil (1.0 mmol), water (5 mL), at room temperature

under air] was applied for reactions of variety of ophenylenediamine and 1,2-diketone with moderate to excellent yield (80-98%).

Table 4: Synthesis of quinoxaline and derivatives by CoFeMnO₄^a

Entry	1,2-diamine	1,2-diketone	Product ^b	Time (min)	Yield ^c (%)
1	NH ₂ NH ₂	o o 2a	N N 3a	10	98

www.jchr.org



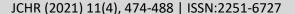


92

0-

1c

www.jchr.org





3h

9
$$Br \longrightarrow NH_2$$
 $O \longrightarrow Br$ $Br \longrightarrow NH_2$ $O \longrightarrow Br$ $Br \longrightarrow NH_2$ $O \longrightarrow Br \longrightarrow NH_2$ $O \longrightarrow Br \longrightarrow NH_2$ $O \longrightarrow Br \longrightarrow NH_2$ $O \longrightarrow O$ $O \longrightarrow$

^aReaction conditions: diketone (1.0 mmol), OPD (1.0 mmol), CoFeMnO₄ catalyst (5 mol %), Water5 mL, RT. ^bAll products were analyzed by IR, ¹H NMR, ¹³C NMR and Mass Spectroscopy. ^cIsolated yields after purification.

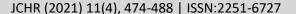
According to experimental results, high reaction rates and yields were obtained with both activated and non-activated benzils (Table 4, entry-1 to 10). Benzils without any substituent and activated benzils with electron-withdrawing substituent are reactive substrates in quinoxaline synthesis and the related reactions went to completion in shorter reaction times. As an example, the reaction of benzil with OPD completed within 10 min giving the desired product in 98% isolated yield (Table 4, entry-1). Non activated benzil with electron donating substituent on the aromatic ring are not reactive substrates in quinoxaline synthesis and related reactions completed in longer reaction times (Table 4 in entry-3).

In the next try for benzimidazole synthesis, instead of benzil, benzaldehyde was reacted with OPD (Scheme 1) at room temperature in aqueous medium in the presence of CoFeMnO4 as a catalyst. Reaction was completed within 10 min with excellent yield in aqueous medium with use of 1mol % of catalyst (reported catalyst) [28-29]. For optimization studies, the reaction of benzaldehyde (1.0 mmol) with OPD (1.0 mmol) in the presence of catalyst at room temperature in aqueous medium has given in the Table 7.

Table 5: Optimization studies for the synthesis of benzimidazole in the presence of CoFeMnO₄^a

	Reaction medium ^b	CoFeMnO ₄	Time	Temperature	Yield ^c
Entry		(mol %)			(%)
1	H_2O	-	10 h	r.t./reflux	Trace
2	C_2H_5OH	-	10 h	r.t./reflux	Trace
3	CH3CN	-	10 h	r.t./reflux	Trace
4	DMF	-	10 h	r.t./reflux	Trace
5	$\mathrm{H}_2\mathrm{O}$	1	5 min	r.t.	93
6	$C_2H_5OH:H_2O$ (50:50)	1	8 min	r.t.	93
7	C_2H_5OH	1	10 min	r.t.	80
8	Acetone	1	20 min	r.t.	81
9	Acetone: H ₂ O (50:50)	1	15 min	r.t.	89

www.jchr.org





10	DMF	1	20 min	r t	80
10	DML	1	20 IIIII	r.t.	80

^aReaction conditions: aldehyde (1.0 mmol), o-phenylenediamine (1.0 mmol), ^bReaction medium (5 mL) ^cIsolated yield

For practical applications of catalysts, the concentration of CoFeMnO₄ for maximum yield of the product in water and the reusability of the catalyst was investigated upon the reaction of benzaldehyde with OPD as the substrates in the presence of the catalyst in aqueous

medium at room temperature. The yield of the product is highest at 1mol % of CoFeMnO₄ catalyst (Table 6). After the first cycle activity of catalyst is decreased with decreasing yield from 93 to 81 % with increased time (Table 7).

Table 6: Optimization of catalyst for benzimidazole synthesis^a

Entry	Catalyst (mol %)	Time (min)	Yield ^b (%)
1	0.2	45	45
2	0.4	25	52
3	0.6	15	75
4	0.8	15	84
5	1.0	10	93
6	1.2	10	93

^aReaction conditions: *o*-phenylenediamine (1.0 mmol), Benzaldehyde (1.0 mmol), Water (5 mL), RT. ^bIsolated yields after purification.

Table 7: Recyclability of catalyst in benzimidazole synthesis

Entry	o-phenylenediamine	Cycle	Time (min)	Yield (%)
		1	10	93
	\sim NH ₂	2	16	92
1		3	18	90
	NH,	4	23	88
		5	24	85
		6	28	81

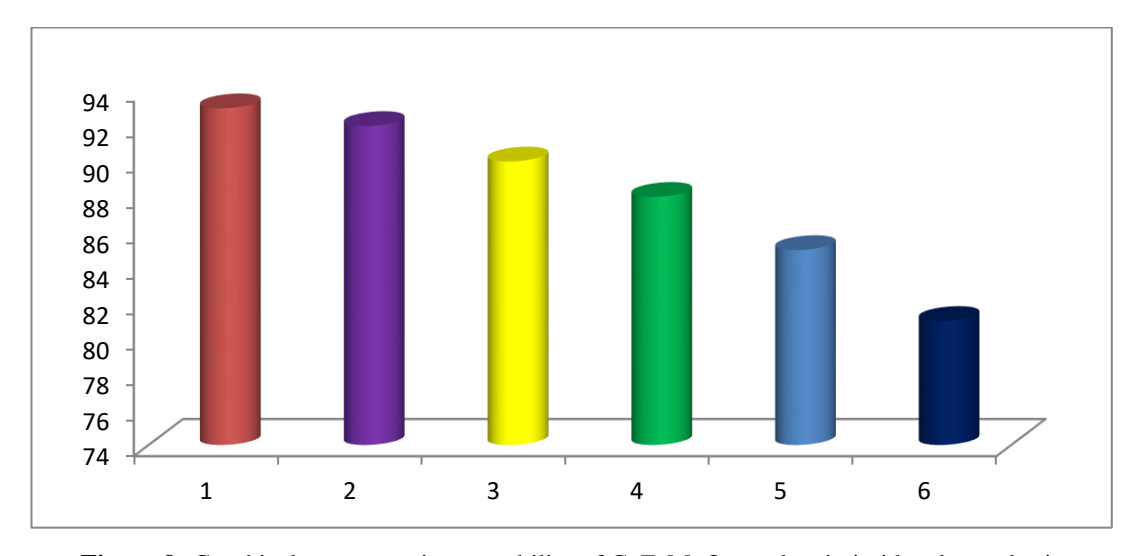
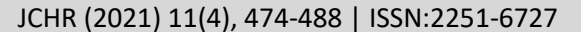


Figure 9: Graphical representation reusability of CoFeMnO₄ catalyst in imidazole synthesis

www.jchr.org





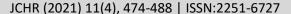
To explore the scope and generality of the catalyst, the optimized protocol was applied for reactions of variety

of aldehydes and o-phenylenediamine with moderate to excellent yield (93-78%).

Table 8: Synthesis of benzimidzoles in aqueous medium by using 1mol % CoFeMnO₄^a

Entry	Aldehyde	Product ^b	Time	Yield ^c
			(Min)	(%)
1	CHO 4a	N N H 5a	10	93
2	CHO OMe 4b	$ \begin{array}{c} N \\ N \\ H \end{array} $ $ \begin{array}{c} OMe \\ 5b \end{array} $	30	83
3	CHO OH 4c	N N N N N N N N N N	25	78
4	CHO OH 4d	N N H	25	80
5	CHO CI 4e	5d CI N H 5e	25	86
6	CHO Cl 4f	$ \begin{array}{c} N \\ N \\ H \end{array} $ $ \begin{array}{c} N \\ T \\ T$	30	88

www.jchr.org





aReaction conditions: aldehyde (1.0 mmol), *o*-phenylenediamine (1.0 mmol), CoFeMnO₄catalyst (1mol %), Water5 mL, RT. bAll products were characterized by IR, ¹H NMR and ¹³C NMR spectroscopy. cIsolated yields after recrystalisation.

Conclusions

In summary, we have demonstrated an efficient, simple, economical and environmentally benign protocol for the synthesis of CoFeMnO₄ and its catalytic applications in the synthesis of quinoxalines and benzimidazole derivatives in an aqueous medium at room temperature. The size of Citrate sol-gel auto combustion synthesized CoFeMnO₄ nanoparticles was characterized by TEM analysis and it was found to be ~37 nm. The crystalline nature of Citrate sol-gel auto combustion synthesized CoFeMnO₄ was analyzed by XRD analysis and found to be simple cubic spinel structure. The CoFeMnO₄ nanoparticles were used as a non-toxic, inexpensive, heterogeneous catalyst in an aqueous medium. It was recycled up to five cycles with some significant loss. Thus, the catalytic protocol developed provides an unprecedented reactivity pattern, an economically attractive and environmentally benign alternative route for the production of medicinally important quinoxaline, benzimidazole and widens the synthesis of related compounds in organic syntheses.

Spectral data of representative compounds (Quinoxaline and derivatives):

3d (Table 6, entry 4): Yellow solid, observed mp 229–230 °C. Lit. mp 228-230 °C. ¹H NMR (CDCl₃, 300

MHz): $\delta_{\rm H}$ (ppm) 7.72–7.88 (m, 6H), 8.30–8.36 (m, 2H), 8.60 (d, 2H, J=8.7 Hz), 9.43 (dd, 2H, J=7.8 Hz, 1.8 Hz). 13 C NMR (CDCl₃, 75 MHz): $\delta_{\rm C}$ (ppm) 122.8, 126.1, 127.7, 129.2, 129.6, 130.4, 132.1, 142.2, 142.2. MS (ESI): m/z 280.

3g (Table 6, entry 7): Yellow Solid, observed mp 218–219 °C. Lit. mp 218-219 °C [38]. ¹H NMR (CDCl₃, 300 MHz): $\delta_{\rm H}$ (ppm) 7.70–7.86 (m, 5H), 8.56 (d, 2H, J=7.8 Hz), 8.67 (dd,1H, J=8.5 Hz, 1.9 Hz), 9.28-9.35 (m, 2H). 9.55 (dd, 1H, J=7.7 Hz, 1.4 Hz). ¹³C NMR (CDCl₃, 75 MHz): $\delta_{\rm C}$ (ppm) 123.8, 126.3, 127.4, 129.6, 129.9, 130.9, 132.2, 132.6, 138.2, 145.1, 152.5, 154.4. MS (ESI): m/z 281.

3j (Table 6, entry 10): White solid, mp 236–238 °C. 1 H NMR (CDCl₃, 300 MHz): $\delta_{\rm H}$ (ppm) 7.73–7.88 (m, 4H), 8.57 (d, 2H, J=8.2 Hz), 8.82-8.84 (m, 1H), 9.26-9.28 (m, 2H), 9.48 (d, 1H, J=7.8 Hz). 13 C NMR (CDCl₃, 75 MHz): $\delta_{\rm C}$ (ppm) 120.7, 122.8, 123.2, 126.8, 127.4, 128.3, 128.4, 129.3, 129.6, 131.4, 131.5, 132.6, 137.5, 139.5, 144.3, 155.6. MS (ESI): m/z 359.

Spectral data of synthesized compounds (Benzimidzole and its derivatives)

2-(4-Chlorophenyl)-1*H*-benzimidazole (Table 10. Entry 6):IR (KBr): v = 3405, 3096, 3050, 2929, 1465, 1239,

www.jchr.org

JCHR (2021) 11(4), 474-488 | ISSN:2251-6727



904, 745 cm⁻¹; ¹H NMR (300MHz,CDCl₃, δ ppm): 5.81 (s,1H),7.14 (d, J = 7.4 Hz, 2H), 7.57 (m, 2H), 7.89 (d, J = 7.1 Hz, 2H), 8.04 (d, J = 8 Hz, 2H),

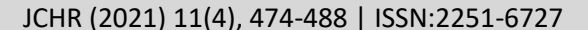
2-(3-Nitrorophenyl)-1*H*-benzimidazole (Table 10 Entry 7): IR (KBr): υ = 3458, 3088, 1527, 1457, 1351, 914, 739 cm⁻¹; ¹H NMR (300 MHz,CDCl₃, δ ppm): 5.61 (s, 1H), 7.25 (m, 2H), 7.55 (m, 2H), 7.71 (t, 2H), 8.06 (d, J = 8 Hz, 1H), 8.21 (d, J = 8 Hz, 1H); Mass Spectrum:m/z 340 (M+), 274, 282.

References

- [1] J. M. Gonçalves, M. N.T. Silva, K. K. Naik, P. Roberto Martins, D. P. Rocha, E. Nossol, R. A. A. Munoz, L. Angnes and C. S. Rout, J. Mater. Chem. A, 2020, DOI: 10.1039/D0TA11129E.
- [2] A. Kruk, M. Schabikowski, M. Mitura-Nowak, T. Brylewski, Physica B: Physics of Condensed Matter, 596 (2020) 412402.
- [3] R. Singh, G. Thirupathi, (2017), Magnetic Spinels Synthesis, Properties and Applications. doi:10.5772/66522.
- [4] M. Kurian, S. Thankachan, Open Ceramics 8 (2021) 100179.
- [5] A. M. El Nahrawy, A. A. Soliman, E. M. M. Sakr, H. A. El Attar, Journal of Ovonic Research Vol. 14, No. 3, May - June (2018)193 – 200.
- [6] I. Gul, W. Ahmed, A. Maqsood, J. Magn. Magn. Mater. 320 (2008) 270–275.
- [7] A. Sutka, G. Mezinskis, Front. Mater. Sci. (2012) 1–14.
- [8] S. Phumying, S. Labuayai, E. Swatsitang, V. Amornkitbamrung, S. Maensiri, Mater. Res. Bull. 48 (2013) 2060–2065.
- [9] J. Wang, F. Ren, R. Yi, A. Yan, G. Qiu, X. Liu, J. Alloy. Compd. 479 (2009) 791–796.
- [10] C. Y. Zhang, X. Q. Shen, J.X. Zhou, M.X. Jing, K. Cao, J. Sol-Gel Sci. Technol. 42 (2007) 95–100.
- [11] N. Kasapoğlu, A. Baykal, Y. Köseoğlu, M. Toprak, Scr. Mater. 57 (2007) 441–444.
- [12] V. D. Kapse, Res. J. Chem. Sci., Vol. 5(8), August (2015) 7-12.

- [13] V.R. Bhagwat, A. V. Humbe, S.D. More, K.M. Jadhav, Materials Science & Engineering B, Volume 248 (2019) 114388.
- [14] Cui Dong, Zhenping Qu, Yuan Qin, Qiang Fu, Hongchun Sun, and XiaoxiaoDuan, ACS Catalysis 9 (8),(2019) 6698-6710.
- [15] Chihao Lin, Dejian Shi, Zhentao Wu, Lingfeng Zhang, Zhicai Zhai, Yingsen Fang, Ping Sun, Ruirui Han, Jiaqiang Wu, Hui Liu, Nanomaterials 2019, 9, 774; doi:10.3390/nano9050774.
- [16] S. Kanagesan, M. Hashim, S. Tamilselvan, N.B. Alitheen, I. Ismail, M.Syazwan, M.M.M. Zuikimi, Digest Journal of Nanomaterials and Biostructures Vol. 8, (2013), 1601 1610.
- [17] S. Hosseini, D. Salari, A. Niaei, F. Deganello, G. Pantaleo, P. Hojati, Journal of Environmental Science and Health, Part A: Toxic/Hazardous Substances and Environmental Engineering, 46:3 (2011) 291-297.
- [18] (a) C. Antonio, P. Giuseppe, M. Nikookar, S. Paolo, S. Leonardo, Z. Stefania, Eur. J. Med. Chem. 37, (2002) 355; (b) Z, Székelyhidi, J. Pato, F, Waczek, P. Banhegyi, B. Hegymegi-Barakonyi, D. Eros, G. Meszaros, F. Hollosy, D. Hafenbradl, S. Obert, B. Klebl, G. Keri, L. Orfi, Bioorg. Med. Chem. Lett. 15, (2005) 3241; (c) G. Fedora, A. Francesca, D. Osvaldo, B. Antonella, G. Antonio, N. Nouri, Bioorg. Med. Chem. 15, (2007) 288.
- [19] (a) B. Gao, D. Xia, Y. Geng, Y. Cheng, L. Wang,
 Tetrahedron Lett. 51, (2010) 1919; (b)T-H. Huang,
 J. T. Lin, Chem. Mater. 16, (2004) 5387; (c) R.
 Bolligarla, S. K. Das, Tetrahedron Lett. 52, (2011) 2496.
- [20] S. Bhattacharya, P. Choudhuri, Curr. Med. Chem. 15, (2008) 1762.
- [21] S. B. Kamble, G. S. Rashinkar, A. S. Kumbhar, K. B. Mote, R. S. Salunkhe, Syn Comm. 42(5), (2012) 756.
- [22] Z. A. Gilani, M. S. Shifa, A. D. Chandio, M. N. Usmani, H. M. N. Ul Huda K. Asghar, S. Aslam, M. Khalid, A. Perveen, J. Ur Rehman, M. Mustaqeem, M. A. Khan, Digest Journal of Nanomaterials and Biostructures Vol. 13, No. 3, (2018), 809 816.

www.jchr.org





- [23] Laleh Saleh Ghadimi, Nasser Arsalani, Iraj Ahadzadeh, Abdollah Hajalilou, Ebrahim Abouzari-Lot, Applied Surface Science, Volume 494, 15 (2019) 440-451.
- [24] P. Vigneshwaran, M. Kandiban, N. Senthil Kumar, V. Venkatachalam, R. Jayavel, I. Vetha Potheher, J Mater Sci: Mater Electron Vigneshwaran, P., Kandiban, M., Senthil Kumar, N., Venkatachalam, V., Jayavel, R., & Vetha Potheher, I, Journal of Materials Science: Materials in Electronics, 27(5), (2016)4653–4658.
- [25] U. Kadam, S. Arde, B. Shirke, R.Pandav, Eur. Chem. Bull., 09 (issue 11) (2020) 361-370.
- [26] R. Kutty, P. Kasturi, J. Jaganath, S. Padmanapan, Y. Lee, D. Meyrick, R. Selvan, Journal of Materials Science: Materials in Electronics, (2018) https://doi.org/10.1007/s10854-018-0366-5.
- [27] (a) S. Venkateswarlu, B. N. Kumar, C. H. Prasad,
 P. Venkateswarlu, N. V. V. Jyothi, Physica B 449,
 67 (2014); (b) S. Venkateswarlu, Y. S. Rao, T. Balaji, B. Prathima, N. V. V. Jyothi, Matter.
 Lett.100, (2013) 241
- [28]. (a) K. Holmberg, Current Opinion in Colloid Interface Sci. 8, 187 (2003); (b) A. Chanda, V. Fokin, Chem. Rev. 109, 725 (2009); (c) L. Gron, A. Tinsley, Tetrahedron Lett40, (1999) 227.
- [29] (a) A. R. Siamaki, B. A. Arndtsen, J. Am. Chem. Soc. 128, (2006) 6050; (b) B. Krishnakumar, R. Velmurugan, S. Jothivel, M. Swaminathan, Catalysis Communications 11, (2010) 997; (c) Y. S. Beheshtiha, M. M. Heravi, M. Saeedi, N. Karimi, M. Zakeri, N. Tavakoli-Hossieni, Synth. Commun. 40, (2010) 1216; (d) N. H. Cano, J. G. Uranga, M. Nardi, A. Procopio, D. A. Wunderlin, A. N. Santiago, Beilstein J. Org. Chem.12, (2016) 2410; (d) S. Ambethkar, V. Padmini, N. Bhuvanesh, Journal of Advanced Research6, (2015) 975.